Large orbit neoclassical transport*

Z. Lin,† W. M. Tang, and W. W. Lee
Princeton Plasma Physics Laboratory, Princeton University, P. O. Box 451, Princeton, New Jersey 08543

(Received 13 November 1996; accepted 16 January 1997)

Neoclassical transport in the presence of large ion orbits is investigated. The study is motivated by the recent experimental results that ion thermal transport levels in enhanced confinement tokamak plasmas fall below the ''irreducible minimum level'' predicted by standard neoclassical theory. This apparent contradiction is resolved in the present analysis by relaxing the basic neoclassical assumption that the ions orbital excursions are much smaller than the local toroidal minor radius and the equilibrium scale lengths of the system. Analytical and simulation results are in agreement with trends from experiments. The development of a general formalism for neoclassical transport theory with finite orbit width is also discussed. © *1997 American Institute of Physics.*
[S1070-664X(97)92705-1]

I. INTRODUCTION

The striking improvement of plasma confinement to neoclassical levels was first theoretically predicted for a reversed magnetic shear configuration[1] and subsequently confirmed in recent tokamak experiments.[2,3] In the so-called enhanced reversed shear (ERS)[2] or negative central shear (NCS)[4] plasmas, the core ion thermal conductivity was actually observed to fall *below* the standard neoclassical level which was widely accepted as the irreducible minimum. The source of this apparent contradiction lies in the fact that the experimental conditions in the ERS regime correspond to situations where the ion poloidal gyroradius ρ_p can be comparable in magnitude or even greater than the local minor radius r and the equilibrium pressure gradient scale length L_p. This violates a basic assumption in the standard neoclassical formalism and establishes the need for a revised theory where ρ_p can be of the same order of magnitude as r and/or L_p. This is accomplished in the present analysis, and the associated analytical and gyrokinetic particle simulation results are shown to be in agreement with key confinement trends observed in ERS plasmas.

The standard neoclassical theory assumption that the kinematic toroidal angular momentum is much smaller than the toroidal angular momentum leads to the ordering, $\rho_p \ll r$. This assumption allows the lowest order distribution function to be a function of the flux surface instead of the drift surface. In addition, the usual assumption that $\rho_p \ll L_p$ allows expansion of the distribution function around a local Maxwellian. However, due to the combination of high central q (safety factor) and small local inverse aspect ratio (r/R_0 with R_0 being the tokamak major radius), the ion poloidal gyroradius (ρ_p) can in fact be larger than the minor radius and comparable to the pressure gradient scale length (L_P) in the ERS regime. Hence, both the trapped particle fraction and the banana width can be significantly modified by the finite minor radius and possibly by the pressure-gradient-driven radial electric field.

In the present analysis, the newly derived form for the neoclassical ion heat conductivity is found to be strongly reduced by finite banana width dynamics in the ERS regime.[5] Important properties which need to be taken into account in an appropriate theoretical model include: (a) ion banana width is nearly constant close to the magnetic axis and (b) counter-moving ions have a minimum trapped fraction and all co-moving ions are trapped. In the usual neoclassical picture, outward ion heat conductivity results from energy flux imbalance between the inward moving slow (lower energy) particles and the outward moving fast (higher energy) particles. When the finite orbit width is taken into account, the outward ion heat conductivity is significantly reduced because these modifications on the fast particles are much stronger than those on the slow particles (i.e., net energy outflow reduced). Therefore, the ion heat conductivity χ_i decreases for smaller minor radius (where orbit effects are strongest). In the following, it will be demonstrated that analytic results from the random-walk type argument and the global gyrokinetic particle simulation using the GNC code[6] yield favorable agreement with the trend from the experimental measurements.

In a more general framework, the development of a neoclassical theory with finite ion banana width treated in the lowest order is discussed. It is found that ion–ion collisions can drive neoclassical particle transport in a general driven steady state. An equilibrium state with no particle flux has been derived using the principle of maximum entropy.

The present investigation is also of interest to the microturbulence studies since they rely on neoclassical theory for the equilibrium distribution function. The usual assumption of a Maxwellian background has to be re-evaluated when $\rho_p \sim L_p$. In the force balance calculation of the equilibrium electrostatic potential, and thus the important parameter $d(E_r B/B_\theta)/dr$, for turbulence suppression[7] from the force balance calculation, the neoclassical poloidal flow is assumed even though it is only valid when $\rho_p \ll L_p$. Furthermore, for electromagnetic turbulence, the use of usual neoclassical expression of bootstrap current has not been justified when $\rho_p \sim L_p$.

This paper is organized as follows. A simplified ion orbit topology analysis in the core regions is presented in Sec. II. The ion heat conductivity is studied both by an analytical

*Paper 2IB1, Bull. Am. Phys. Soc. **41**, 1442 (1996).
†Invited speaker.

calculation and the gyrokinetic particle simulation in Sec. III. Sec. IV presents a general formalism for the neoclassical transport theory with finite orbit width dynamics treated in the lowest order. Finally, Sec. V contains conclusions and discussions.

II. ORBIT TOPOLOGY

The fast ion orbit in an axisymmetric magnetic field has been extensively investigated[8,9] for the confinement of energetic particles produced by neutral beam injection. These studies emphasized the loss regions due to the plasma wall. In this section, a simpler analysis of thermal ion orbit in the plasma core region is presented. Since the classical transport is excluded in the present studies, the guiding center orbit theory is adequate.

In an axisymmetric system, the guiding center trajectories are defined by the conservations of magnetic moment, μ, energy ε, and toroidal canonical angular momentum, p,

$$\mu B+\frac{1}{2}mv_{\parallel}^2+e\Phi=\varepsilon, \quad R(mv_{\zeta}+eA_{\zeta})=p, \tag{1}$$

where B is the magnetic field, m is the particle mass, e is the charge state, v_{ζ} is toroidal components of the parallel velocity $v_{\parallel}$, Φ is electrostatic potential, and R is the distance from the center line. ζ denotes toroidal angle in the plasma current direction. The toroidal magnetic vector potential A_{ζ} is related to the poloidal magnetic field B_{θ}

$$\mathbf{B}_{\theta}=\nabla\times\mathbf{A}_{\zeta},$$

and the poloidal flux Ψ

$$\Psi=-RA_{\zeta}\equiv-hR_0A_{\zeta},$$

where $h=1+\epsilon\cos\theta$, and $\epsilon=r/R_0$ with R_0 being major radius and r the minor radius.

In analyzing the dynamics of interest, it is convenient to consider a high aspect ratio torus with concentric flux surfaces and a constant q profile with constant Φ. The poloidal flux is $\Psi=r^2B_0/2q$. The orbit equations then take the following form,

$$\frac{\mu B_0}{h}+\frac{1}{2}mv_{\parallel}^2=\text{const}, \quad v_{\parallel}-\frac{\Omega r^2}{2qR_0}=\text{const}, \tag{2}$$

where $\Omega\equiv eB_0/mc$. The focus here is on the orbit topology of single energy ($mv^2/2$) particles at a reference point of minor radius r and poloidal angle $\theta=0$ (magnetic field minimum). The usual definition of a trapped particle is one for which $v_{\parallel}=0$ somewhere along the orbit. The banana width Δ_b and trapped fraction f_t are determined by the behavior of barely trapped particles with $v_{\parallel}=0$ at the inside mid-plane ($\theta=\pi$).

$$\frac{1}{2}mv_{\parallel}^2+\frac{\mu B_0}{1+\epsilon}=\frac{\mu B_0}{1-\epsilon},$$

and

$$v_{\parallel}-\frac{\Omega r^2}{2qR_0}=-v_{\parallel}-\frac{\Omega(r-\Delta_b)^2}{2qR_0}.$$

In the limit of $\Delta_b\ll r$,

$$f_t\equiv|v_{\parallel}|/v=\sqrt{2\epsilon}, \quad \Delta_b=\sqrt{8}\rho q/\epsilon^{1/2}, \tag{3}$$

where $\rho=v/\Omega$.

Now consider the critical region, $\Delta_b\sim r$, where the familiar expressions given by Eq. (3) are invalid. First, note that the banana width increases when the reference point moves toward the magnetic axis. Hence, care must be taken to satisfy the basic constraint that the orbit excursion cannot be larger than the local minor radius at the outermost point of the orbit. For a small value of r, it is possible for the guiding center to pass through the magnetic axis at a local minor radius. Then, the banana width is equal to this local minor radius, i.e., it becomes the maximum banana width of the system. Second, the trapped orbit in this region is now redefined as one in which a particle cannot travel around the poloidal angle. Because the guiding center drift does not cancel at each half of the orbit, this orbit can have a large radial excursion. Thus, it makes a large contribution to diffusion even though its parallel velocity $v_{\parallel}$ may not change sign along the orbit. Near the magnetic axis, all co-moving particles ($v_{\parallel}>0$) are trapped because the guiding center drift velocity is larger than the poloidal component of the parallel velocity. The counter-moving particle ($v_{\parallel}<0$) has a minimum velocity space pitch angle at the trapped-passing boundary.

In order to quantify the deviation from the usual neoclassical transport estimates, we begin by considering barely trapped counter-moving particles which are initially located at the magnetic axis with parallel velocity $v_{\parallel 0}<0$. Such particles have zero parallel velocity at the inside mid-plane ($\theta=\pi$) and later intercept the outer mid-plane ($\theta=0$) at minor radius $r=\Delta_{max}$ with parallel velocity $v_{\parallel}>0$. The orbit equations are,

$$\frac{1}{2}mv_{\parallel 0}^2+\mu B_0=\frac{\mu B_0}{1-r_1/R_0}, \tag{4}$$

$$v_{\parallel 0}=-\frac{\Omega r_1^2}{2qR_0}, \tag{5}$$

and

$$\frac{\mu B_0}{1-r_1/R_0}=\frac{1}{2}mv_{\parallel}^2+\frac{\mu B_0}{1+r/R_0}, \tag{6}$$

$$-\frac{\Omega r_1^2}{2qR_0}=v_{\parallel}-\frac{\Omega r^2}{2qR_0}. \tag{7}$$

In the high aspect ratio limit, the maximum banana width Δ_{max} and the minimum trapped fraction f_{min} are,

$$\Delta_{max}=\frac{(1+\sqrt{5})}{2^{1/3}}(q^2\rho^2R_0)^{1/3}, \tag{8}$$

$$f_{min}\equiv\frac{|v_{\parallel 0}|}{v}=\left(\frac{2q\rho}{R_0}\right)^{1/3}. \tag{9}$$

It is then clear that at minor radius Δ_{max}, the orbit topology begins to deviate from the usual neoclassical picture. For $r<\Delta_{max}$, the banana width and trapped fraction are roughly constant and independent of local ϵ. Furthermore, the ion collisionality parameter, $\nu_i^*\equiv\epsilon^{-3/2}\sqrt{2}qR_0/(v_{th}\tau_i)$ with

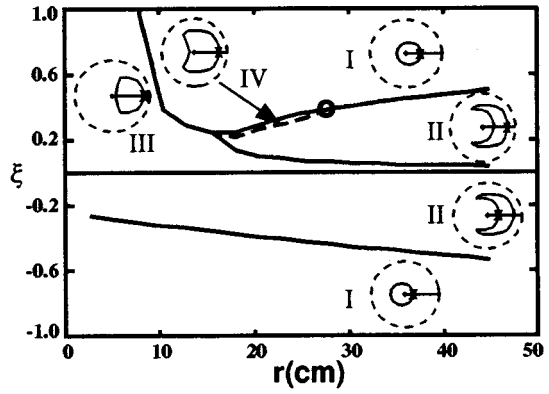

FIG. 1. Trapped-passing boundary in pitch angle space ξ vs. minor radius r. *I* represents passing regime and *II* trapped regime. In regime *III*, parallel velocity of a trapped particle does not change sign. In regime *IV*, parallel velocity of a passing particle changes sign.

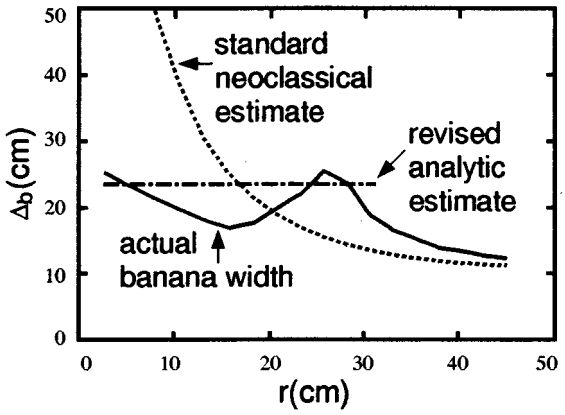

FIG. 2. Banana width Δ_b vs. minor radius r.

$v_{th} \equiv \sqrt{2T/m}$ being the thermal velocity and τ_i the ion Braginskii time, is finite and falls well within the banana regime for the ERS plasmas parameters provided the actual trapped fraction is properly taken into account.

The negative magnetic shear has a favorable effect on orbit topology. Assume q profile,

$$q(r) = q_0 \left(\frac{r}{a} \right)^{-n}. \tag{10}$$

Then the maximum banana width and the minimum trapped fraction are,

$$\begin{aligned} \Delta_{max} &= \alpha [(n+2)^2 q_0^2 \rho^2 R_0 a^{2n}]^{1/(2n+3)}, \\ f_{min} &= \left[(n+2) \frac{q_0 \rho}{R_0} \left(\frac{a}{R_0} \right)^n \right]^{1/(2n+3)}, \end{aligned} \tag{11}$$

where α is a numerical constant and $\alpha \sim 2^{1/(n+2)}$ when $n \gg 1$.

Equation (12) shown that the dependence of maximum banana width on particle energy is weaker with negative magnetic shear. Specifically, if $q \sim r^{-n}$, then $\Delta_{max} \sim \varepsilon^{1/(2n+3)}$. This interesting scaling was first pointed out by Stix.[8] The consequence of this property will be further explored in Sec. III.

Equation (1) has been solved numerically for experimental parameters of Tokamak Fusion Test Reactor (TFTR) ERS plasmas. The trapped-passing boundary of thermal particles in pitch angle $\xi = v_\parallel / v$ and local minor radius r space is shown in Fig. 1. The maximum orbit excursion occurs at the trapped-passing boundary and is defined as the banana width. The dependence of the banana width on the local minor radius is shown in Fig. 2. When the minor radius of the reference point decreases, there are significant differences between the actual banana width and the standard neoclassical estimate even well before the orbit topology transition point (the empty circle in Fig. 1). This is due to the variation of local aspect ratio along the particle trajectory. The results of the trapped fraction are presented in Fig. 3. Near the magnetic axis, the trapped fraction increases as r decreases because more and more co-moving ($v_\parallel > 0$) particles can not encircle the magnetic axis due to the small poloidal component of parallel velocities.

III. ION HEAT CONDUCTIVITY

The collisional transport in the core regime is the result of three different processes, namely, classical transport or gyroradius diffusion, Pfirsch-Schlüter transport by orbit diffusion of passing guiding centers, and banana transport by orbit diffusion of trapped guiding centers. The usual estimates for the diffusion of passing (untrapped) particle guiding center orbits (Pfirsch-Schlüter transport) and for gyroradius diffusion (classical transport) remain valid in the core ERS regime. However, the diffusion of trapped particles (banana transport) is expected to be dramatically changed due to the finite orbit width dynamics. In order to properly analyze such effects, the standard neoclassical formalism has been revised by relaxing the constraint that the ion orbital excursions must be smaller than the local minor radius and the equilibrium scale lengths of plasma. Results from gyrokinetic particle simulations based on this new formalism are strikingly different from the usual banana regime estimate and in reasonable agreement with experimental trends observed in ERS plasmas. Before displaying these numerical

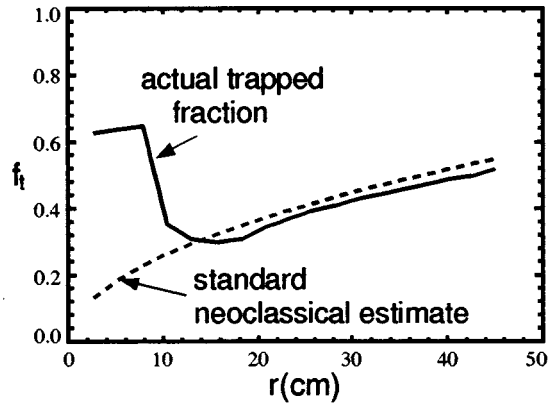

FIG. 3. Trapped fraction f_t vs. minor radius r.

results, it is appropriate to first present useful analytical estimate for these important large orbit modifications. Significant physical insight can be gained from estimates of the ion energy flux Q in the banana regime using the standard random walk approximation, i.e.,

$$Q=\alpha\int_0^\infty f_t\frac{\Delta^2}{\tau_{eff}}\frac{\partial f}{\partial r}\frac{mv^2}{2}4\pi v^2 dv, \tag{12}$$

where f is the ion guiding center distribution function, Δ is the random walk step size and $\tau_{eff}=f_t^2/\nu$ is the effective collision time with ν being the ion collision frequency, and α is a simple constant which normalizes Q to the standard neoclassical banana transport value calculated in the limit of small banana width. Since the temperature gradient scale length (L_T) in ERS plasmas is much larger than the actual ion orbit width, local Maxwellian distribution can be assumed. Then the ion thermal conductive transport from Eq. (12) becomes

$$Q=\alpha\frac{\kappa_t nT}{\tau_i}\int_0^\infty\frac{\Delta^2}{f_t}e^{-x}\left(x-\frac{3}{2}\right)dx \tag{13}$$

with normalized energy $x=(v/v_{th})^2$. This results was obtained with a Lorentz collision model of the form, $C=\nu(v)\hat{\mathbf{L}}$, where $\hat{\mathbf{L}}$ is the pitch angle scattering operator,

$$\hat{\mathbf{L}}=\frac{1}{2}\frac{\partial}{\partial\xi}(1-\xi^2)\frac{\partial}{\partial\xi},$$

and the collision frequency

$$\nu(v)=\frac{3}{4}\frac{(2\pi)^{1/2}}{\tau_i}\left(\frac{v_{th}}{v}\right)^3,$$

where the ion Braginskii time is defined,

$$\tau_i=\frac{4}{3}\pi^{1/2}\frac{n_i e^4\ln\Lambda}{m^{1/2}T^{3/2}},$$

with n_i being the ion number density and ln Λ the Coulomb logarithm.

It is useful here to introduce an expression for the minor radius transition point for particles with thermal energy; i.e., Eq. (9) gives

$$r_0\equiv\Delta_{max}(v=v_{th})=\frac{(1+\sqrt{5})}{2^{1/3}}(q^2\rho_i^2R_0)^{1/3}, \tag{14}$$

where $\rho_i=v_{th}/\Omega$. $r_0\sim 20$ cm for the typical ERS plasma parameters of the Tokamak Fusion Test Reactor (TFTR).[2] The normalized particle energy now becomes $x=(\Delta_{max}/r_0)^3$ with the normalized minor radius defined by

$$x_0\equiv\left(\frac{r}{r_0}\right)^3. \tag{15}$$

When $x\geq x_0$, the particles reach their maximum banana width, and the orbit topology becomes different from the usual neoclassical picture . Therefore, the velocity space integral in Eq. (13) can be separated into two parts. Low energy particles ($x<x_0$) have the conventional step size, $\Delta=q\rho/\sqrt{r/R_0}$, and trapped fraction, $f_t=\sqrt{r/R_0}$, while high energy particles ($x>x_0$) have constant step size, $\Delta=q\rho/\sqrt{\Delta_{max}/R_0}$, and trapped fraction, $f_t=\sqrt{\Delta_{max}/R_0}$. The integral in Eq. (13) becomes

$$\begin{aligned}I&\equiv\int_0^\infty\frac{\Delta^2}{f_t}e^{-x}\left(x-\frac{3}{2}\right)dx,\\&=\left(\int_0^{x_0}+\int_{x_0}^\infty\right)\frac{\Delta^2}{f_t}e^{-x}\left(x-\frac{3}{2}\right)dx,\\&=I_1+I_2.\end{aligned}$$

I_1 represents low energy particles contribution with the usual step size $\Delta=q\rho/\sqrt{r/R_0}$ and trapped fraction $f_t=\sqrt{r/R_0}$,

$$\begin{aligned}I_1&=\frac{\rho_i^2q^2}{\epsilon^{3/2}}\int_0^{x_0}e^{-x}x\left(x-\frac{3}{2}\right)dx,\\&=\frac{\rho_i^2q^2}{2\epsilon^{3/2}}[1-e^{-x_0}(2x_0^2+x_0+1)].\end{aligned}$$

I_2 represents contribution from high energy particles which reach maximum banana width. A simple treatment is assuming constant step size $\Delta=q\rho/\sqrt{r_{min}/R_0}$ and trapped fraction $f_t=\sqrt{r_{min}/R_0}$. This guarantees a smooth transition from I_1 to I_2,

$$\begin{aligned}I_2&=\frac{\rho_i^2q^2}{(r_0/R_0)^{3/2}}\int_{x_0}^\infty e^{-x}x^{1/2}\left(x-\frac{3}{2}\right)dx,\\&=\frac{\rho_i^2q^2}{\epsilon^{3/2}}x_0^2e^{-x_0}.\end{aligned}$$

Ion energy flux from Eq. (13) becomes,

$$Q=\alpha\frac{\kappa_t nT}{\tau_i}\frac{\rho_i^2q^2}{2\epsilon^{3/2}}[1-e^{-x_0}(x_0+1)]. \tag{16}$$

Accordingly, our analytical estimate for the finite-orbit-modified neoclassical ion heat conductivity in the banana regime becomes:

$$\chi_i^{ba}=\chi_i^{neo}[1-e^{-x_0}(x_0+1)], \tag{17}$$

where $\chi_i^{neo}=0.66\epsilon^{-3/2}q^2\rho_i^2/\tau_i$ is the standard neoclassical ion heat conductivity.[10,11] The correction factor, $f\equiv 1-e^{-x_0}(x_0+1)$, is shown in the Fig. 4. It is also of interest to note here that negative magnetic shear has a favorable effect on the orbit topology. The contribution from the high energy particles to the integral in Eq. (13) decreases

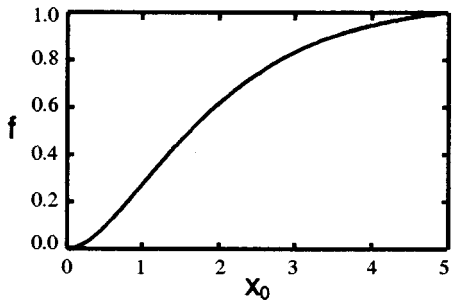

FIG. 4. Finite orbit width correction to standard neoclassical χ_i

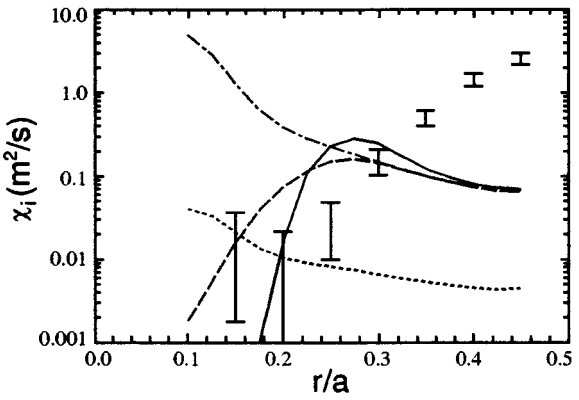

FIG. 5. Comparison of theoretical χ_i to experimental data.

when the dependence of the maximum banana width on energy is weaker. Therefore, the negative magnetic shear helps to reduce the neoclassical ion heat conductivity in the core region.

From the previous section, it is found that both ion banana width and trapped fraction are roughly constant near the magnetic axis. One will then expect that the ion heat conductivity to remain constant in the core regime. However, χ_i^{ba} is found to decrease with smaller r. The physical picture is as follows. The outward ion heat conductivity results from energy flux imbalance between the inward moving slow (lower energy) particles and the outward moving fast (higher energy) particles. In core plasmas region, outward ion heat conductivity is significantly reduced because the finite orbit width modification on the fast particles is much stronger than that on the slow particles (i.e., net energy outflow reduced). This physical picture is consistent with the fact that the two terms in the integrand in Eq. (13) tend to cancel when integrated.

The total ion collisional heat conductivity is given by

$$\chi_i = \chi_i^{ba} + \chi_i^{ps} + \chi_i^{cl} \tag{18}$$

with χ_i^{ba} being the focus of our present analysis, $\chi_i^{ps} = 1.58(1-f_t)q^2\rho_i^2/\tau_i$ representing the Pfirsch-Schlüter transport,[10] and $\chi_i^{cl} = \rho_i^2/\tau_i$ being the classical transport.[12] In the core region of ERS plasmas, the ion heat conductivity is close to the Pfirsch-Schlüter level which is in turn much larger than the classical transport because of the high central q. Comparisons of the theoretical estimates for χ_i vs. representative TFTR ERS results are shown in Fig. 5. In contrast to the usual neoclassical values which strongly increase with decreasing minor radius, the finite orbit width analytic results from Eq. (17) and numerical results from Eq. (12) indicate a decreasing trend. This is in reasonable agreement with the earlier published TFTR ERS results[2] and even more strikingly with recent more comprehensive data analysis of the same representative discharge. Note also that the experimental trend begins to track the Pfirsch-Schlüter level when χ_i^{ba} properly becomes negligibly small at smaller plasma radii.

It is of interest to examine how sensitive χ_i depend on the form of collision operator. Here we study a model like-species pitch angle scattering operator[10] which takes the form of $C = \nu(v)\hat{\mathbf{L}}$ with

$$\nu(v) = \frac{3}{4}\frac{(2\pi)^{1/2}}{\tau_i}\left(\frac{v_{th}}{v}\right)^3 \phi\left(\frac{v}{v_{th}}\right), \tag{19}$$

where the Maxwellian integral is defined by

$$\phi(y) = \frac{2}{\sqrt{\pi}}\int_0^y e^{-t}\sqrt{t}dt.$$

Qualitative agreement is obtained with both collision operators. Furthermore, both pitch angle scattering operators do not conserve momentum and do not have the energy scattering. The property of momentum conservation will have important effect on particle transport. Because the dominant contribution to particle flux is from relatively low energy particles, the absence of momentum conservation is expected to have minimal effect on heat flux. Another situation where the momentum conservation is not important is the impurity transport since the dominant collision process is between the impurity and the main ion species. Assuming both impurity and main ion species are in banana regime, the impurity particle diffusivity can be estimated as,

$$D_I = 0.73\epsilon^{-3/2}\frac{\rho_I^2 q^2}{\tau_I}[1 - e^{-x_0}(2x_0+1) + \sqrt{\pi x_0}(1-\phi(x_0))]. \tag{20}$$

The Lorentz collision operator is used in this random walk calculation. From Eq. (20), D_I reaches a constant level at the magnetic axis $(x_0 \to 0)$.

In order to validate the results from the random walk analysis, fully toroidal particle simulations using the gyrokinetic neoclassical code (GNC)[6] have been carried out. The finite orbit width dynamics is retained by keeping the drift term in solving the following drift kinetic equation,

$$(v_\parallel \hat{\mathbf{b}} + \mathbf{v}_d)\cdot\nabla f - C(f) = 0, \tag{21}$$

where $\mathbf{v}_d$ is the guiding center drift velocity. Let $f \equiv f_0 + \delta f$ with f_0 defined by

$$v_\parallel \hat{\mathbf{b}}\cdot\nabla f_0 - C(f_0) = 0. \tag{22}$$

The governing equation is

$$(v_\parallel \hat{\mathbf{b}} + \mathbf{v}_d)\cdot\nabla \delta f - C(\delta f) = \mathbf{v}_d\cdot\boldsymbol{\kappa} f_0, \tag{23}$$

where $\boldsymbol{\kappa} \equiv -\nabla \ln f_0$. Note that if we ignore the drift term on the left hand side of Eq. (23), the standard neoclassical result is recovered. This nonlinear gyrokinetic delta-f formalism[13,14] allows a rigorous treatment of both finite ion orbit width dynamics and a Fokker-Planck collision operator conserving momentum and energy. Since the temperature gradient scale length in ERS plasmas is much larger than the actual ion orbit width, the usual expansion around a local Maxwellian is justified and thus allows the use of a noise-reduction δf scheme. In the simulations, the guiding center distribution function is calculated by integrating the exact marker particles trajectories. The energy flux is calculated by

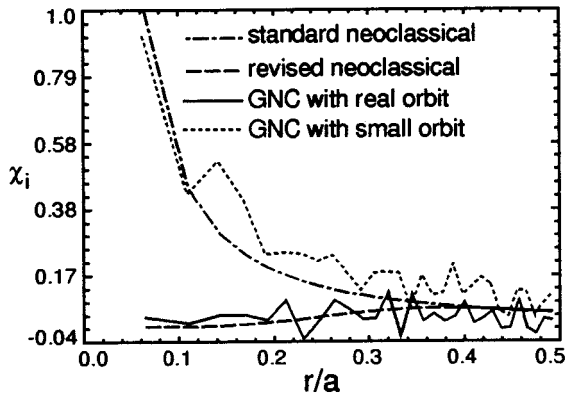

FIG. 6. Comparison of analytic χ_i to GNC simulation results, in arbitrary unit.

the standard procedure of multiplying each particle energy by its radial drift velocity. Thus both banana and Pfirsch-Schlüter diffusion are measured. The calculated ion thermal transports are not sensitive to the initial loading of the particles or the initial conditions. The simulation results, which are presented in Fig. 6, support the trends from the random walk analysis shown in Fig. 5 and indicate that the ion heat conductivity decreases to roughly the Pfirsch-Schlüter level in the ERS core regime. Moreover, if the key full ion orbit width dynamics are suppressed, the simulations recover the standard neoclassical results.

IV. EQUILIBRIUM STATE OF LIKE-SPECIES COLLISIONS

An appropriate steady state distribution function is needed for any attempt of a rigorous treatment of the neoclassical transport with finite orbit width dynamics. In the banana regime, the steady state distribution function is a function of constants of motion. This distribution function in standard neoclassical theory can be any local Maxwellian with arbitrary density, temperature, and toroidal rotation profile. However, when the cross-field drift is treated in the lowest order equation, flux function is not a constant of motion and the steady state distribution function has to be reformulated. To be specific, the time scale considered is the ion–ion collision time. On this time scale, an equilibrium state is defined as a time-independent solution of an isolated system, while a steady state is defined as time-independent distribution function maintained by external sources. Therefore, the equilibrium state is a special case of the steady state with zero external source, and no transport is driven by ion–ion collisions in an equilibrium state.

The equilibrium state with finite orbit width can be readily obtained using the principle of maximum entropy, and is found to be a global shifted-Maxwellian in an isolated system,

$$f=\exp(a+b\varepsilon+cp), \tag{24}$$

where a, b and c are numerical constants corresponding to the total number of particles, energy and toroidal rotation. This equilibrium state is characterized by a uniform temperature and toroidal rotation, and no transport driven by ion–ion collisions. The characteristic density has the form, $n(\Psi)=\exp(\alpha\Phi+\beta\Psi)$, with Ψ being the poloidal magnetic flux and α, β numerical constants. Because the density can be of arbitrary profile, the associated electrostatic potential can be of any form subject to the constraint of ion radial force balance. Thus, the equilibrium state derived here contains the orbit squeezing effect associated with the shear of the radial electric field.[15] For this constant temperature equilibrium, the poloidal flow can be shown to be zero, and the orbit squeezing effect accordingly does not change the neoclassical flows. The orbit squeezing effect on a general driven steady state (i.e. non-equilibrium state) is still a topic of ongoing debate.[16,17] Furthermore, when electron dynamics are considered in this model, it is found that the bootstrap current and ambipolar particle flux are consistent with the usual neoclassical results for any value of ρ_n/L_n.

In a general driven system, the steady state is the solution to a variational problem of minimum collisional entropy production subject to the constrains of external sources. Since it is not a zero entropy production state, transport can be driven by ion–ion collisions. In the case of constant temperature considered here, this means particle flux can be driven even though like-species collisions conserve momentum. This is a result of the conservation of toroidal angular momentum and its amplitude can be estimated accordingly; i.e.,

$$\Gamma_i/\Gamma_{neo}\sim\delta\epsilon\frac{\mu_i}{\chi_i^{neo}}\left(\frac{m_i}{m_e}\right)^{1/2}\frac{\rho_p}{R_0}\frac{\rho_p}{L_n}, \tag{25}$$

where μ_i is the neoclassical viscosity and Γ_{neo} is the usual neoclassical ambipolar flux. Here δ measures the degree of deviation from the equilibrium state and is defined as

$$\delta=-\frac{\kappa_u}{\kappa_n}\frac{u_\zeta}{u_{neo}}, \tag{26}$$

where u_ζ is the toroidal mass flow, $\kappa_u=-d\ln u_\zeta/dr$, $\kappa_n=-d\ln n/dr$, and $u_{neo}=\rho_p\kappa_n v_{th}/2$. This scaling is similar to that obtained in very early classical transport studies[18] of particle flux arising from like-species collisions. Since δ is very small in most ERS plasmas of interest, it follows that steep density gradients do not have a strong effect on the ion

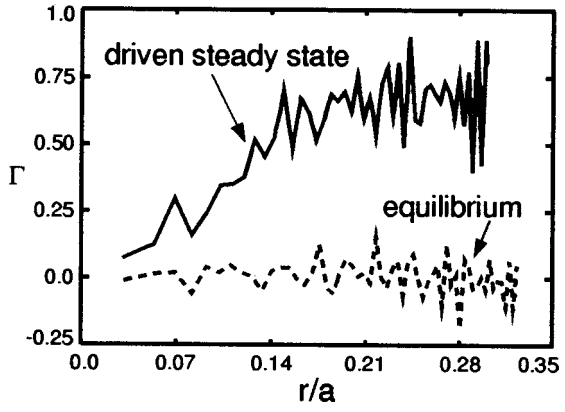

FIG. 7. Particle flux Γ (arbitrary unit) vs. minor radius r.

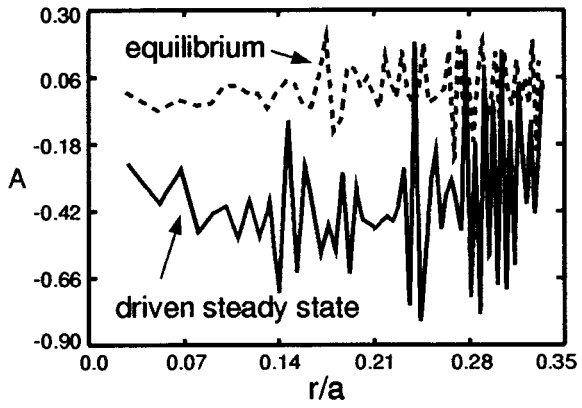

FIG. 8. Toroidal angular momentum flux A (arbitrary unit) vs. minor radius r.

heat conductivity. The orbit squeezing effects arising from the shear of the effective toroidal flow (cE_r/B_θ) driven by the radial electric field associated with the steep density gradient is small because the scale length of this flow is, although comparable to ρ_p, much larger than the actual ion banana width. These results further support the conclusion from the random walk calculations and the gyrokinetic simulation results in the previous section.

The GNC code is utilized to test this interesting prediction, i.e., ion–ion collision can drive neoclassical particle transport. Two simulations have been carried out where all parameters are identical except for the density profiles. One density profile is the equilibrium state for a constant q magnetic configuration,

$$n_1(r) \sim e^{-r^2/l^2},$$

where l is a characteristic length. The other profile is not an equilibrium,

$$n_2(r) \sim e^{-r^3/l^3}.$$

Both profiles are solutions to the drift kinetic equation in the usual neoclassical limit. Figures 7 and 8 show that both particle and toroidal angular momentum fluxes are driven by ion–ion collisions when the profile is not in the equilibrium state.

V. CONCLUSIONS AND DISCUSSION

The neoclassical ion heat conductivity in ERS regime is shown to be strongly reduced by properly including finite banana width effects into the theory. Analytical and simulation results are found to be in agreement with trends observed in the experiments. When the effect of finite ion banana width is retained in the neoclassical theory, it is found that ion–ion collisions can drive particle transport in a general driven steady state. An equilibrium state with no particle flux has been derived.

Only the effect of finite ion banana width is studied in this paper. The effect of finite electron orbit width and associated finite trapped fraction introduces nonvanishing bootstrapped current on the magnetic axis.[19,20] However, this effect in a simple ion-electron plasma is limited to a very small region ($r_0 < 1$ cm for the electron using the TFTR ERS plasmas parameters). On the other hand, the finite ion banana width effect may modified the standard neoclassical bootstrap current in the presence of the ion temperature gradient. This modification will be investigated in our future studies.

ACKNOWLEDGMENTS

This work was supported in part by an appointment to the U.S. Department of Energy (USDoE) Fusion Energy Postdoctoral Research Program administered by the Oak Ridge Institute for Science and Education, and by USDoE Contract No. DE-AC02-76-CH03073.

[1] C. Kessel, J. Manickam, G. Rewoldt, and W. M. Tang, Phys. Rev. Lett. **72**, 1212 (1994).
[2] F. M. Levinton, M. C. Zarnstorff, S. H. Batha, M. Bell, R. E. Bell, R. V. Budny, C. Bush, Z. Chang, E. Fredrickson, A. Janos, J. Manickam, A. Ramsey, S. A. Sabbagh, G. L. Schmidt, E. J. Synakowski, and G. Taylor, Phys. Rev. Lett. **75**, 4417 (1995).
[3] E. J. Strait, L. L. Lao, M. E. Mauel, B. W. Rice, K. H. B. T. S. Taylor, M. S. Chu, E. A. Lazarus, T. H. Osborne, S. T. Thompson, and A. D. Turnbull, Phys. Rev. Lett. **75**, 4421 (1995).
[4] L. L. Lao, K. H. Burrell, T. S. Casper, V. S. Chan, M. S. Chu, C. B. Forest, R. J. Groebner, F. L. Hinton, Y. Kawano, E. A. Lazarus, Y. R. Lin-Liu, M. E. Mauel, W. H. Meyer, R. L. Miller, G. A. Navratil, T. H. Osborne, C. L. Rettig, G. Rewoldt, B. W. Rice, B. W. Stallard, E. J. Strait, T. S. Talor, W. M. Tang, A. D. Turnbull, R. E. Waltz, and the DIII-D Team, Plasma Phys. Controlled Fusion **38**, 1439 (1996).
[5] Z. Lin, W. M. Tang, and W. W. Lee, Phys. Rev. Lett. **78**, 456 (1997).
[6] Z. Lin, W. M. Tang, and W. W. Lee, Phys. Plasmas **2**, 2975 (1995).
[7] T. S. Hahm and K. H. Burrell, Phys. Plasmas **2**, 1648 (1995).
[8] T. H. Stix, Plasma Phys. **14**, 367 (1972).
[9] J. A. Rome and Y.-K. M. Peng, Nucl. Fusion **19**, 1 (1979).
[10] F. L. Hinton and R. D. Hazeltine, Rev. Mod. Phys. **48**, 239 (1976).
[11] R. D. Hirshman and D. J. Sigmar, Nucl. Fusion **21**, 1079 (1981).
[12] S. I. Braginskii, *Reviews of Plasma Physics* (Consultants Bureau, New York, 1965), Vol. 1.
[13] W. W. Lee, Phys. Fluids **26**, 556 (1983).
[14] S. E. Parker and W. W. Lee, Phys. Fluids B **5**, 77 (1993).
[15] R. D. Hazeltine, Phys. Fluids B **1**, 2031 (1989).
[16] K. C. Shaing, C. T. Hsu, and R. D. Hazeltine, Phys. Plasmas **1**, 3365 (1994).
[17] F. L. Hinton, J. Kim, Y. B. Kim, A. Brizzard, and K. H. Burrell, Phys. Rev. Lett. **72**, 1216 (1994).
[18] C. L. Longmire and M. N. Rosenbluth, Phys. Rev. **103**, 507 (1956).
[19] P. A. Politzer, Bull. Am. Phys. Soc. **40**, 1787 (1995).
[20] K. C. Shaing and R. D. Hazeltine, Bull. Am. Phys. Soc. **41**, 1459 (1996).